American Mineralogist, Volume 92, pages 281–288, 2007

Hardness, toughness, and modulus of some common metamorphic minerals

DONNA L. WHITNEY,[1,*] MARGARET BROZ,[2] AND ROBERT F. COOK[2,†]

[1]Department of Geology and Geophysics, University of Minnesota, Minneapolis, Minnesota 55455, U.S.A.
[2]Department of Chemical Engineering and Materials Science, University of Minnesota, Minneapolis, Minnesota 55455, U.S.A.

ABSTRACT

Studies of the hardness and toughness of minerals have historically focused on minerals of the Mohs scale, although, with the exceptions of quartz, orthoclase, and calcite, Mohs phases are not common rock-forming minerals. We report new hardness (H), toughness (resistance to fracture, K_{IC}), and indentation modulus (E^*) data obtained by microhardness and depth-sensing indentation (DSI, or nanoindentation) experiments for common metamorphic minerals: sillimanite, kyanite, andalusite, garnet, quartz, and orthoclase feldspar. Because the experimental techniques involve indentation-induced cracking as well as depth-sensing indentation, the new data set can be used to investigate a range of plastic behavior for minerals in the crust and mantle.

The three Al_2SiO_5 polymorphs have similar H values (~10–12 GPa): kyanite has the largest values and andalusite the smallest. These values are similar to that of quartz (~12 GPa) and greater than that of orthoclase (~7 GPa). Garnet H values vary with composition: for grossular, $H \sim 13$ GPa, and for almandine-pyrope, $H \sim 15$ GPa. Although H values for the minerals we analyzed span a range of ~10 GPa, most fracture toughness values are between 1–1.8 MPa·m$^{1/2}$. Garnet is much harder than Al_2SiO_5, but has a similar to slightly lower K_{IC} (grossular ~1.2 MPa·m$^{1/2}$; almandine-pyrope ~1.4 MPa·m$^{1/2}$; andalusite 1.8 MPa·m$^{1/2}$; sillimanite 1.6 MPa·m$^{1/2}$); kyanite K_{IC} is difficult to measure owing to the ease with which kyanite cleaves. Garnet has properties similar to those of cubic zirconia (ZrO_2), which we measured as a reference. Another reference mineral, periclase (MgO), has the lowest H (~5 GPa) and the highest K_{IC} (~4 MPa·m$^{1/2}$) of minerals we measured. Among the silicates, E^* varies significantly from orthoclase (~89 GPa) to quartz (~117 GPa) to garnet (245–260 GPa), and Al_2SiO_5 has intermediate values: kyanite ~ 186–253 GPa, sillimanite ~ 207 GPa, andalusite ~ 232 GPa.

Keywords: Fracture toughness, hardness, indentation, metamorphic minerals, modulus, mechanical properties, garnet, quartz, Al_2SiO_5

PHYSICAL PROPERTIES OF METAMORPHIC MINERALS

Mineral properties such as hardness, resistance to fracture, and elastic modulus can be used to understand the brittle and ductile behavior of metamorphic rocks during deformation. Although much attention has focused on the physical properties of rheologically significant minerals such as quartz, feldspars, and calcite, much less is known about the mechanical properties of important metamorphic phases such as the Al_2SiO_5 polymorphs, which are widely used for evaluating pressure-temperature (P-T) conditions of metamorphism. Our study was motivated in part by the need for a systematic physical properties data set that can be used to model geological phenomena, such as the brittle fracture of minerals during decompression in the crust or mantle (e.g., garnet: Whitney et al. 2000) or during earthquake-generating faulting at or near the Earth's surface (quartz: Goldsby et al. 2004). In addition, physical properties are relevant for interpreting seismic velocity data and for calculating lattice strain associated with ionic substitution and trace-element partitioning in solid-solution phases (e.g., garnet: van Westrenen et al. 1999). All of our data were collected at room temperature, so are not directly applicable to the deformation of minerals during metamorphism, but nevertheless represent a fundamental data set that is a starting point for understanding the material properties of important metamorphic phases.

SAMPLES AND METHODS

We determined hardness, toughness, and modulus for the three Al_2SiO_5 polymorphs (andalusite, kyanite, sillimanite), two garnet compositions (Ca-rich and Fe-Mg-rich), quartz, orthoclase, cubic zirconia (ZrO_2), and periclase (MgO). With the exception of the cubic zirconia and periclase samples, which were synthetic, all samples were natural minerals from rocks, and the garnets, andalusite, and sillimanite were gem-quality. The periclase was polycrystalline MgO, with an average grain size of 10 μm, and represents the same material used by Cook and Liniger (1992). All other samples were single crystals. Our characterization of these minerals included their composition, crystal system, indentation plane (if known), hardness determined by two methods—microindentation and depth-sensing indentation (DSI, or nanoindentation)—toughness, and indentation modulus (Table 1). All samples were analyzed on highly polished surfaces obtained by polishing with fine diamond or alumina suspensions (0.2–0.3 μm).

For microindentation experiments, we used a Vickers square-pyramid diamond probe, and for DSI, we used a Berkovich triangular-pyramid diamond probe. For most minerals, the indented plane in our experiments was a cleavage plane or crystal face. For highly anisotropic minerals such as kyanite, we indented different planes to capture the range of hardness values. Details of the experimental technique and

* E-mail: dwhitney@umn.edu
† Current address: National Institute of Standards and Technology, Gaithersburg, Maryland 20899, U.S.A.

TABLE 1. Characteristics and mechanical properties of the analyzed minerals

Mohs no.	Mineral	Chemical formula	Crystal system	Orientation of indented plane	Microhardness (GPa)	DSI Hardness (GPa)	Toughness (MPa·m$^{1/2}$)	Modulus (GPa)
5–5.5	Kyanite	Al_2SiO_5	triclinic	(001)	–	14.8 ± 1.4	–	186 ± 8
6	Orthoclase	$KAlSi_3O_8$	monoclinic	(101)	6.9 ± 0.7	9.1 ± 0.6	1.1 ± 0.4	89 ± 7
6–6.5	Periclase*	MgO	isometric		5.3 ± 1.0	9.4 ± 1.4	3.9 ± 0.8	233 ± 12
6.5–7	Sillimanite	Al_2SiO_5	orthorhombic	(010)	11.0 ± 2.7	15.9 ± 1.5	1.6 ± 1.5	207 ± 6
6.5–7	Andalusite	Al_2SiO_5	orthorhombic	(001)	9.8 ± 1.5	11.6 ± 0.3	1.8 ± 0.5	232 ± 6
7	Quartz	SiO_2	hexagonal	(0001)	12.1 ± 1.1	14.5 ± 0.4	1.5 ± 0.3	117 ± 3
7	Kyanite	Al_2SiO_5	triclinic	(100)	12.1 ± 3.3	14.5 ± 2.2	–	227 ± 30
7	Kyanite	Al_2SiO_5	triclinic	(010)	11.9 ± 1.7	16.3 ± 1.6	–	253 ± 19
7–7.5	Garnet-1‡	$(Fe,Mg)_3Al_2Si_3O_{12}$	isometric		15.1 ± 1.2	19.4 ± 0.6	1.4 ± 0.3	245 ± 8
7–7.5	Garnet-2‡	$Ca_3Al_2Si_3O_{12}$	isometric		13.2 ± 0.8	18.8 ± 0.2	1.2 ± 0.2	260 ± 8
8–8.5	CZ†	ZrO_2	isometric		16.7 ± 1.7	19.5 ± 0.6	1.5 ± 0.3	256 ± 6

Note: Uncertainties listed are one standard deviation.
* Polycrystalline.
† Cubic zirconia.
‡ Garnet compositions: Garnet-1 = Almandine (Fe) 46 mol%; Spessartine (Mn) 2 mol%; Pyrope (Mg) 46 mol%; Grossular (Ca) 6 mol%; Garnet-2 = Almandine 4 mol%; Spessartine 0 mol%; Pyrope 0 mol%; Grossular 95 mol%; Andradite ($CaFe^{3+}$) 1 mol%.

calculation of material properties were described in Broz et al. (2006) and are briefly summarized here.

In the microindentation experiments, hardness, H, was calculated from $H = P/2a^2$, where P is the peak load applied during the indentation experiment (here 2 N), and a is the semi-diagonal of the post-indentation residual contact impression, such that H is an estimate of the mean supported contact stress (Tabor 1956) (Fig. 1a). The length a was measured from contact impression images. In the DSI experiments, load and displacement of the indenter into the material surface were measured during the load-unload contact cycle (here to 100 mN over 200 seconds). Hardness in this case was calculated from the maximum applied load divided by an instantaneous contact area calculated from the maximum displacement and the initial unloading stiffness (Oliver and Pharr 1992) (Fig. 1b).

The results of the two hardness techniques can differ, as the parameters used to calculate contact area in the DSI test were determined by calibration of the indenter profile and DSI instrument stiffness to the modulus of a reference material (silica glass) at large contact depths. This procedure typically underestimates the contact area, particularly at small contact depths in stiff, hard materials, and as the tip-rounding effects become significant (Thurn and Cook 2004).

Fracture toughness, K_{IC}, was calculated from the length of surface traces of radial cracks (Cook and Pharr 1990) produced by the Vickers indenter in the microindentation experiment:

$$K_{IC} = 0.022\left(\frac{E}{H}\right)^{1/2}\frac{P}{c^{3/2}}$$

where E is the modulus and c is the radial crack length measured from the contact impression center (Lawn et al. 1980; Anstis et al. 1981; Morris and Cook 2005). E was determined from DSI experiments, and c was measured from images of the cracks (Fig. 1a). As expected for materials of differing H, K_{IC}, and E (Cook and Pharr 1990), the size of the indentation and the length and type of cracking associated with indentation varied widely among the minerals tested (Fig. 2).

Elastic modulus was determined using DSI, and calculated from the unloading stiffness and the contact area at peak load, compensating for the elastic deformation of the diamond indenter (Oliver and Pharr 1992; Broz et al. 2006). In this paper, we report the indentation modulus, E^*, which, for elastically isotropic materials, is equal to the plane-strain modulus, $E^* = E/(1 - \nu^2)$, where E and ν are the isotropic Young's modulus and Poisson's ratio of the material, respectively (Vlassak and Nix 1993). Given the typical experimental scatter in indentation crack-length measurements and the uncertainty in the numerical coefficient (Anstis et al. 1981; Morris and Cook 2005), the difference between E^* and E in the above toughness equation was neglected.

RESULTS

Hardness

Hardness values are systematically lower for the microhardness measurements compared to the DSI values (Table 1; Fig. 3). This finding is consistent with results of a previous study (Broz et al. 2006) and with comparison of reported microhardness and DSI values for materials tested by both techniques (e.g., quartz: Evans 1984; Goldsby et al. 2004).

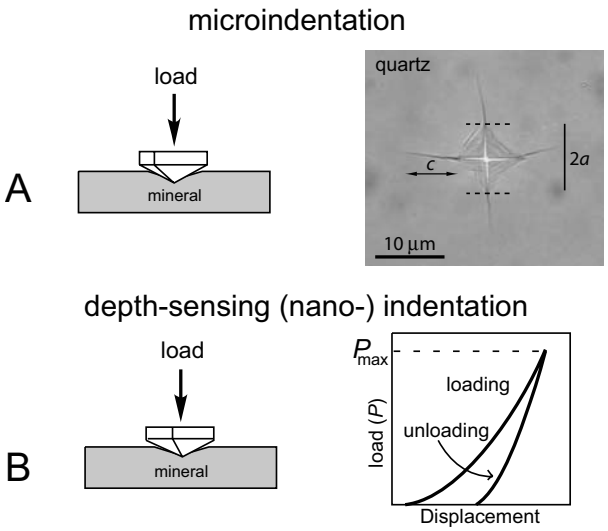

FIGURE 1. (**a**) Sketch showing the indentation experiment and result for microhardness (Vickers), and (**b**) depth-sensing indentation and parameters used to calculate hardness and modulus.

The Vickers hardness of quartz has been determined in previous studies (Westbrook 1958; Brace 1963; Hartley and Wilshaw 1973; Evans 1984; Darot et al. 1985; Masuda et al. 2000). With the exception of Masuda et al. (2000), who determined a load/area value of 8.2 GPa, typical values reported by these studies are ~12 GPa, consistent with our microhardness result for quartz (Table 1). Our DSI result of ~14.5 GPa is similar to the upper limit of the range determined by Goldsby et al. (2004) using DSI (12–14 GPa). Similarly, our calculated microhardness for periclase (5.3 ± 1 GPa) is intermediate between reported microhardness values of 4.5–7.7 GPa (Cook and Pharr 1990; Cook and Liniger 1992; Cook et al. 1994). Our DSI hardness values for periclase are also similar to published DSI values for single crystals (e.g., Cáceras et al. 2003) and to single-crystal microhardness values (Cook and Liniger 1992). As DSI tests generate very small contact impressions, within a single grain, comparison with single-crystal values for MgO are more appropriate.

For cubic zirconia, we determined a microhardness of ~17

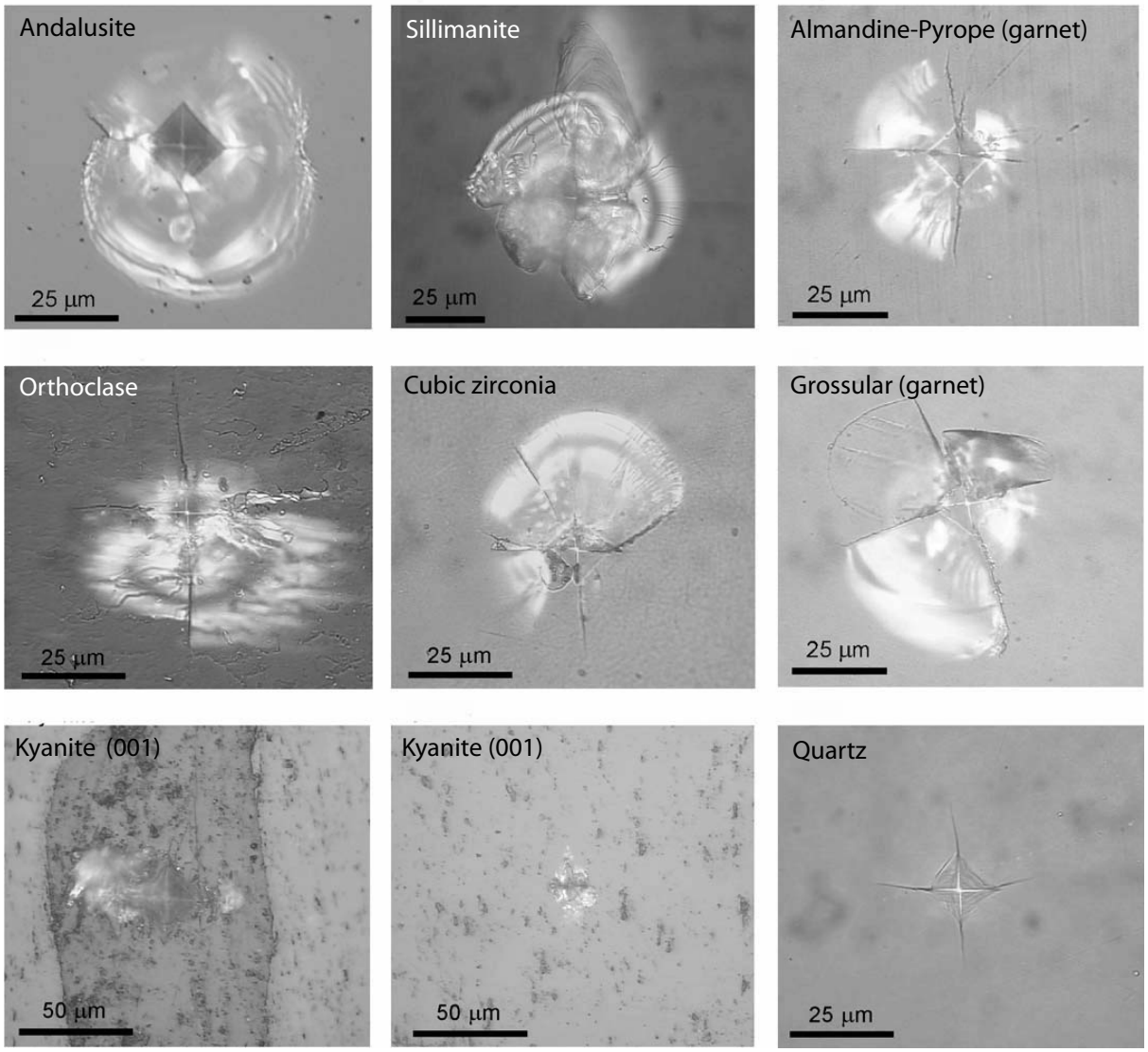

FIGURE 2. Vickers indentations at 2 N load.

GPa, similar to room-temperature literature values for pure cubic zirconia (e.g., Farber et al. 1998) and Y-bearing zirconia (Cook and Pharr 1990). These data from minerals with known hardness suggest that our results for less-studied minerals are likely to be reasonable.

Orthoclase is one step below quartz on the Mohs scale (Mohs number = 6, compared to 7 for quartz), but its indentation hardness (~7 GPa) is significantly less than that of quartz. This finding illustrates that minerals with similar Mohs numbers, particularly those in the range of 6–8, may vary considerably in indentation hardness (Fig. 4). For example, hardness values for periclase (Mohs number = 6–6.5), andalusite (6.5–7), sillimanite (6.5–7), kyanite in the (010) and (100) directions (7), and garnet (7–7.5) range from ~5 GPa to 15 GPa.

Fe-Mg-rich garnets (almandine-pyrope) are harder than quartz by several GPa (Table 1; Fig. 3). The difference between quartz and garnet DSI hardness is even greater than for the microhardness values: the quartz DSI hardness is ~14.5 GPa, whereas the DSI hardness for almandine-pyrope is ~19 GPa. Although cubic zirconia (ZrO_2) and almandine-pyrope have similar hardness values within experimental uncertainty for both microhardness and DSI measurements, cubic zirconia exhibits a greater hardness than grossular-rich garnet (Table 1).

Garnets also vary somewhat in their material properties as a function of composition. For example, we compared the properties of grossular-rich garnet (Grs_{95}, with 4 mol% almandine and 1 mol% andradite components) and an almandine-pyrope solid solution ($Alm_{46}Sps_2Prp_{46}Grs_6$). The grossular-rich garnet had a smaller microhardness (13.2 ± 0.8 GPa) compared to the almandine-pyrope (15.1 ± 1.2 GPa), although the DSI results for the two garnets were more similar (Grs: 18.8 ± 0.2 GPa; Alm-Prp: 19.4 ± 0.6 GPa) (Table 1). The microhardness data differ from

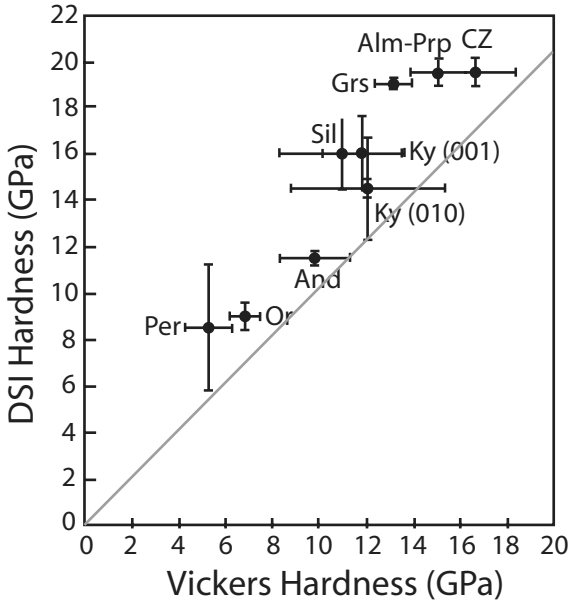

FIGURE 3. Comparison of hardness measurements for microhardness (Vickers) and depth-sensing indication (DSI). Alm-Prp = almandine-pyrope garnet; And = andalusite; CZ = cubic zirconia; Grs = grossular garnet; Ky = kyanite; Or = orthoclase; Per = periclase (MgO); Sil = sillimanite.

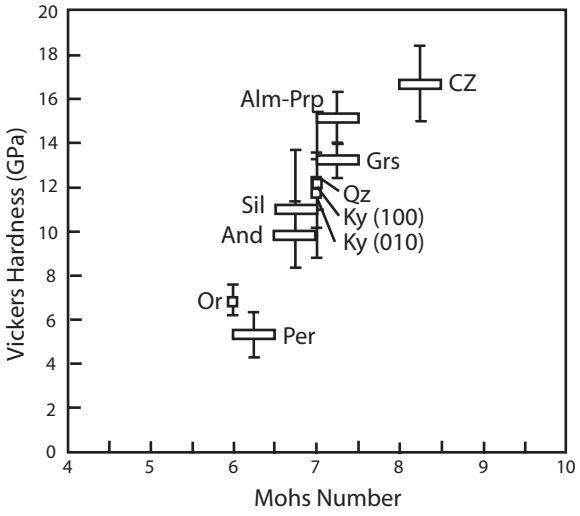

FIGURE 4. Vickers-hardness results compared to numbers on the Mohs scale (scratch resistance). Data for minerals with a reported range of Mohs numbers are shown by a rectangle spanning the range; data for minerals with a single Mohs number are shown by a square. Mohs number for garnet is variably reported as ranging from 6–8, but most typical reported values are 7–7.5.

those reported in Karato et al. (1995); in that study, grossular had the largest room temperature *H* value of the garnets analyzed (~28 GPa), including pyrope, spessartine, almandine-pyrope-grossular, almandine-pyrope-spessartine, and yttrium aluminate garnet (YAG) (~19–26 GPa).

The large uncertainty in *H* values for the Al_2SiO_5 polymorphs reflects their variable indentation behavior. Triclinic kyanite is famous for its variability in scratch resistance as a function of crystallographic direction, and is an excellent example of the consequences of low symmetry for a mineral's Mohs number. Andalusite and sillimanite, which are both orthorhombic, also displayed variable behavior on indentation, and therefore exhibited large uncertainties in their microhardness values. All three polymorphs have Vickers *H* values of ~10–12 GPa, with a larger range for DSI values (12–16 GPa). For both techniques, andalusite gave the smallest value for *H* among the three polymorphs.

Toughness

The toughness values determined by microindentation are a measure of the resistance of the material to fracture. Despite the ~10 GPa difference in hardness, from the hardest to the least hard of the silicates measured, the measured toughness values were similar (~1–1.8 MPa·m$^{1/2}$) (Fig. 5). Quartz and garnet displayed similar toughness values (within uncertainty) of ~1.4 MPa·m$^{1/2}$. The toughness of the oxide (ZrO_2) was also in this range. In contrast, the polycrystalline periclase (MgO), with smaller hardness than the silicates measured, had the greatest toughness (~4 MPa·m$^{1/2}$; Table 1), in part owing to the polycrystalline nature of the analyzed material (Cook and Liniger 1992). Crack lengths

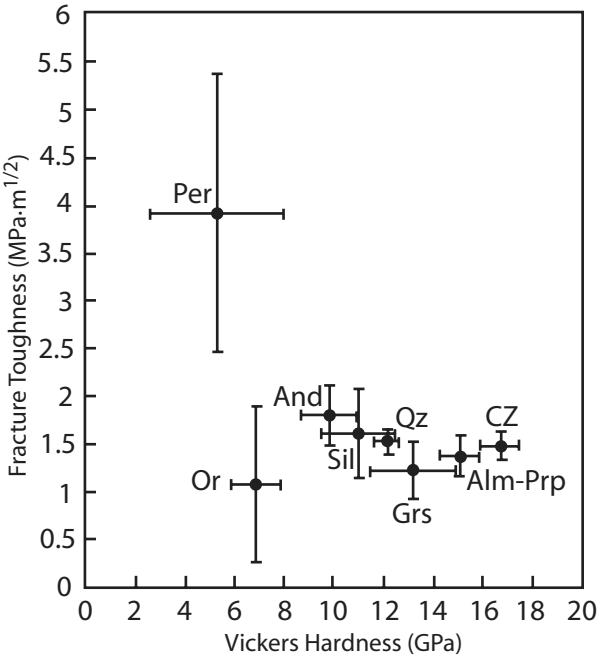

FIGURE 5. Comparison of fracture-toughness values and microhardness. Minerals representing a wide range of Vickers hardness have similar fracture toughness.

and contact diagonals in these experiments were ~6 × longer than the average grain size of 10 µm. Our measured K_{IC} is at the small end of values reported in the literature for polycrystalline MgO (Clarke et al. 1966; Kessler et al. 1974; Rice et al. 1981). Literature values for single-crystal K_{IC} for periclase are ~3 MPa·m$^{1/2}$ (Mecholsky et al. 1976), but still greater than the

values we measured for silicates.

It was not possible to obtain an accurate toughness measurement for any of the three kyanite orientations, even on the same plane. We investigated the effect of indenter orientation on (100) kyanite, as there was a marked change in crack length and contact impression shape as a function of the angle between the diagonals and the cleavage planes. We optimized this angle to resolve the clearest and most consistent contact impression.

We obtained a toughness value for sillimanite, but the variable fracture behavior for that mineral resulted in a large uncertainty in the result (1.6 ± 1.5 MPa·m½). Andalusite had more consistent fracture behavior on indentation (Fig. 6), and yielded the largest fracture toughness value of the silicates we measured (1.8 ± 0.5 MPa·m^{½}). Even so, within the level of uncertainty, andalusite fracture toughness was not significantly different from that of quartz.

Modulus

The modulus measurements were made on the crystal faces and cleavage planes listed in Table 1. One orientation was measured for each crystal, with the exception of kyanite, for which measurements were made on the (001), (010), and (100) faces. Quartz and orthoclase had the smallest E^* values of the minerals measured, and these values (117 ± 3 GPa for quartz, 89 ± 7 GPa for orthoclase) were significantly smaller than values for Al_2SiO_5 and garnet (186 to 260 GPa, Table 1).

All single-crystal minerals tested are elastically anisotropic, and Young's modulus (for example) varies in direction within the crystal. For example, ZrO_2 is stiff in the <100> directions and compliant in the <110> directions (Ingel and Lewis 1988). The stress and strain fields generated during indentation are extremely anisotropic and inhomogeneous, leading to the sampling of the Young's modulus of a mineral in many orientations during indentation and giving rise to an orientation-averaged indentation modulus (Vlassak and Nix 1993). The measured indentation moduli are compared here with the predicted plane-strain modulus of the isotropic polycrystalline aggregate of the relevant minerals; this is the best first-estimate for the indentation modulus of an anisotropic material (Vlassak and Nix 1993), and allows for the most uniform comparison between measurement and prediction of the range of mineral systems examined here.

The compilation of Bass (1995) provided values for the calculated bulk modulus, K, and the shear modulus, G, for isotropic polycrystals for most of the minerals examined here. The related isotropic Young's modulus and Poisson's ratio are given by $E = 9KG/(3K + G)$ and $\nu = (3K - 2G)/2(3K + G)$, respectively, allowing an estimate of the appropriately direction-weighted indentation modulus to be obtained from $E^* = E(1 - \nu^2)$. Ingel and Lewis (1988) provided the isotropic-polycrystal Young's modulus and Poisson's ratio of ZrO_2, allowing E^* to be obtained directly. Comodi et al. (1997) provided the polycrystalline bulk modulus of kyanite (cf. Yang et al. 1997; Winkler et al. 2001), from which E^* can be obtained by $E^* = 3K(1 - 2\nu)/(1 - \nu^2)$, using the value of $\nu = 0.25$ that is typical for many minerals.

Comparison of the measured indentation modulus with the predicted isotropic plane-strain modulus for the minerals is shown in Figure 7, along with the value for the isotropic glassy fused silica ($E^* = 74.4$ GPa) that was used for the DSI instrument calibration. This value compares well with the value of 74.9 GPa, given in Bass (1995) which was calculated from the bulk and shear moduli. Most of the measured values are within ± 10% of the estimated value, with some notable exceptions. The value of MgO (periclase), based on our experiments is 233 GPa, smaller than the value of 320 calculated from bulk and shear moduli and measured values for polycrystalline MgO (e.g., 305 GPa, Chung and Lawrence 1964). Similarly, our measured value for quartz is 117 GPa, which is greater than the value of 96 GPa calculated from bulk and shear moduli. Both of these values are significantly greater than published values for E of natural quartz in sandstone (72.2 ± 2.9 GPa; Frischbutter et al. 2000) measured by neutron time-of-flight diffraction. As Frischbutter et al. (2000) noted, E results for quartz sandstone will be lower than theoretical values

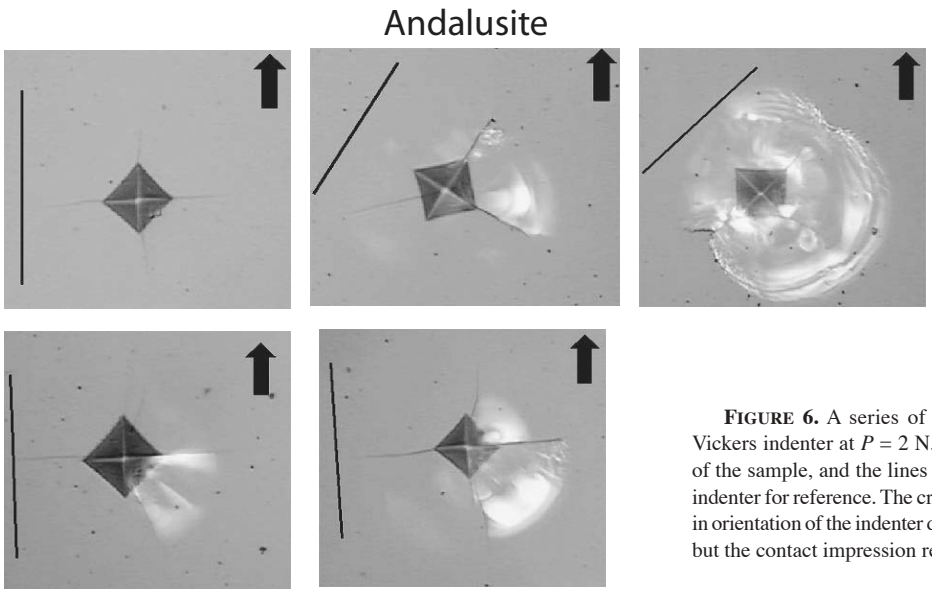

FIGURE 6. A series of indentations on andalusite using a Vickers indenter at $P = 2$ N. The arrows indicate the orientation of the sample, and the lines indicate one diagonal of the Vickers indenter for reference. The cracking pattern changes with variation in orientation of the indenter diagonal with respect to the andalusite, but the contact impression remains the same size (~20 μm).

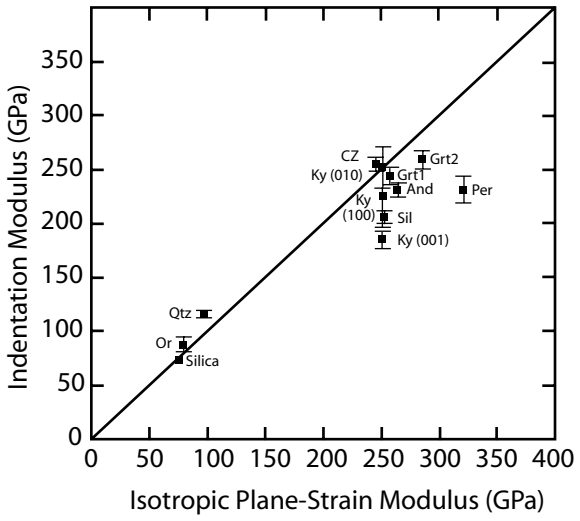

FIGURE 7. Comparison of indentation modulus results from this study with isotropic plane-strain modulus values predicted for literature values of single-crystal elastic constant measurements. CZ = cubic zirconia (ZrO_2). References for literature values are in the text.

of *E* predicted from the properties of single quartz crystals owing to the effects of pores, grain boundaries, impurities, and other microstructural features in the polycrystalline sandstone.

Predictions of the indentation modulus of garnet, using the isotropic polycrystal bulk and shear moduli scheme given above, and the calculated values reported by Bass (1995) from measured single-crystal elastic moduli, suggest a moderate dependence of *E** on composition. End-member values range from 243 GPa for andradite to 284 GPa for grossular, with solid-solution values falling in this range. Our results for almandine-pyrope and almandine-pyrope-grossular solid solutions also fall into this range and are similar to the predicted values (Table 1): 260 GPa ($Alm_4Grs_{95}Adr_1$) compared to 284 GPa (Grs_{99}, from Bass 1995), and 245 GPa ($Alm_{42}Sps_1Prp_{47}Grs_{10}$) compared to 256 GPa (interpolated from $Alm_{64}Sps_{11}Prp_{22}Grs_1Adr_2$ and $Alm_{16}Prp_{73}Adr_4Uvr_6$, Bass 1995).

Literature values for *E* for almandine-pyrope and almandine-pyrope-grossular solid solutions vary widely: e.g., 257 ± 20 GPa (Prp_{60}) and 590 ± 40 GPa (Prp_{84}) for almandine-pyrope (van Westrenen et al. 1999), and 585 ± 35 GPa ($Alm_{31}Prp_{56}Grs_{13}$) and 680 ± 50 GPa ($Alm_9Prp_{72}Grs_{19}$) (van Westrenen et al. 2000). Our results of 245 ± 8 GPa ($Alm_{42}Sps_1Prp_{47}Grs_{10}$) and 260 ± 8 GPa ($Alm_4Grs_{95}Adr_1$) (Table 1) are similar to the van Westrenen et al. (1999) Prp_{60} modulus, but significantly lower than the other values. Poisson's ratio effects generate differences on the order of 6% between *E* and *E**. The major difference in results likely reflects the different methods by which Young's modulus values were predicted. In the van Westrenen et al. (1999, 2000, 2001) studies, Young's modulus was calculated from theoretical considerations related to lattice strain induced by ionic substitution in a crystallographic site (see Discussion).

Our measured indentation modulus values for the Al_2SiO_5 polymorphs, with the exception of the kyanite (001) plane, are similar within the limits of the uncertainties: ~225 GPa. Kyanite (100) and (010) measurements have very large uncertainties owing to the variable behavior of kyanite during indentation experiments. In all cases, the measured *E** value was less than the predicted value (Fig. 7), although the measured value for kyanite (010), 253 GPa, is similar to the value of 250 GPa predicted from bulk-modulus measurements. These new data are potentially useful for understanding phase transformations and for microstructural models of Al_2SiO_5 deformation behavior.

DISCUSSION

The microhardness (Vickers) indentation experiments in this study were designed to induce fracture in the minerals. Other indentation studies of silicates—e.g., quartz, garnet—have investigated plastic deformation without fracturing (Karato et al. 1995; Masuda et al. 2000). For example, in the Masuda et al. (2000) study of quartz, Vickers indentation experiments were carried out at room temperature and 98 mN load, and did not produce fractures. Similarly, the Karato et al. (1995) study of garnets was designed to investigate physical properties and deformation behavior relevant to mantle rheology. Our study is relevant to a range of plastic behavior in minerals, as we obtained toughness data from indentation-induced cracking during microhardness testing, and modulus data from the depth-sensing indentation experiments. Both methods provide data for calculating hardness.

Our results show that minerals with a wide range of hardness values have similar fracture toughness, and this finding suggests that many silicates will have similar brittle behavior with respect to crack propagation. In calculations of conditions required for crack propagation in materials, cracks are predicted to grow when the stress-intensity factor is equal or greater than the fracture toughness. The stress-intensity factor can be calculated from crack characteristics, Young's modulus, and Poisson's ratio. In Whitney et al. (2000), garnet fracture-toughness estimates of ~2 $MPa \cdot m^{1/2}$, based on data from YAG, were too large, but calculation of Young's modulus (~242 GPa) from literature values for bulk and shear moduli gave results within the uncertainty of measurements for the pyrope-almandine (245 ± 8 GPa). The conclusions of that study—that cracks will propagate at the corners of mineral inclusions in garnet during decompression even if there is no major volume expansion of inclusions or any significant decompression—are not changed by the results in the new data set.

Values for *H* and fracture toughness for the Al_2SiO_5 polymorphs are approximately similar to values for quartz (Table 1). These results may indicate that quartz and the Al_2SiO_5 polymorphs behave similarly during brittle deformation, but, owing to the variable behavior of the Al_2SiO_5 phases during indentation, additional studies are needed before Al_2SiO_5 deformation textures in metamorphic rocks can be usefully compared with coexisting quartz, for which the flow laws are better known.

Elastic constants such as modulus are important for geochemical, mineralogical, geophysical, and materials science and engineering applications. For example, because garnet is an important phase in the mantle, lower continental crust, and subducted oceanic lithosphere, there have been many measurements of the elastic properties (bulk modulus, shear modulus) of silicate garnet over a wide range of compositions and pres-

sures for both single crystals and polycrystalline samples using various methods (Soga 1967; Wang and Simmons 1974; Goto et al. 1976; Isaak and Graham 1976; Weaver et al. 1976; Babuska et al. 1978; Leitner et al. 1981; Bass 1986, 1989; Webb 1989; Yegeneh-Haeri et al. 1990; O'Neill et al. 1991; Chai et al. 1997; Conrad et al. 1999; Gwanmesia et al. 2000; Pavese et al. 2001; Wang and Ji 2001; Jiang et al. 2004). There is a similarly large collection of literature on rare-earth-oxide garnets (e.g., YAG) because of their industrial uses. In applications in mineral physics, structural geology, and engineering, elastic constants are used for dislocation models and microstructural models of crack propagation. In geochemistry and mineralogy, modulus can be used to understand the strain on a crystal lattice induced by ionic substitution, and therefore is necessary for calculations of partition coefficients.

As described in the previous section, there is a major discrepancy between our measured and calculated modulus values for garnet, and literature values calculated from theoretical considerations of ionic substitution on crystallographic sites in garnet (van Westrenen et al. 1999, 2000, 2001). Our values overlap with the low end of *E* values in van Westrenen et al. (1999) for intermediate pyrope-grossular solid solutions (~260–270 GPa), but are extremely different from the more pyrope-rich compositions investigated by van Westrenen et al. (1999) (580–680 GPa). These discrepancies indicate that *E* values for crystallographic sites are significantly different from the Young's modulus of the crystal and, therefore, should not be used to infer *E* for the crystal. We have confidence in our values for garnet *E* because calculations relating bulk, shear, and Young's modulus using literature data for the first two elastic properties are consistent with *E* values in the range of ~250 GPa.

This new systematic data set can be used to evaluate relative and absolute physical properties of major rock-forming minerals in metamorphic rocks. The data have applications for studies of crustal deformation, including brittle behavior of garnet during exhumation of deep crustal rocks and fracture of quartz-rich rocks during seismic events.

ACKNOWLEDGMENTS

This work was funded by NSF grant EAR-0106673 to D. Whitney and by a Grant-In-Aid from the University of Minnesota to R. Cook.

REFERENCES CITED

Anstis, G.R., Chantikul, P., Marshall, D.B., and Lawn, B.R. (1981) Evaluation of indentation techniques for measuring fracture toughness: I. Direct crack measurements. Journal of the American Ceramic Society, 64, 533–538.

Babuska, V., Fiala, J., Kumazawa, M., and Ohno, I. (1978) Elastic properties of garnet solid-solution series. Physics of the Earth and Planetary Interiors, 16, 157–176.

Bass, J.D. (1986) Elasticity of uvarovite and andradite garnets. Journal of Geophysical Research, 91, 7505–7516.

——— (1989) Elasticity of grossular and spessartine garnets by Brillouin spectroscopy. Journal of Geophysical Research, 94, 7621–7628.

——— (1995) Elasticity of minerals, glasses, and melts in mineral physics and crystallography. In T.J. Ahrens, Ed., A Handbook of Physical Constants, 2. American Geophysical Union, Washington, D.C.

Brace, W.F. (1963) Behavior of quartz during indentation. Journal of Geology, 71, 581–595.

Broz, M.B., Cook, R.F., and Whitney, D.L. (2006) Microhardness, toughness, and modulus of Mohs scale minerals. American Mineralogist, 91, 135–142.

Cáceras, D., Vergara, I., and González, R. (2003) Microstructural characterization of MgO thin films grown by radio-frequency sputtering: target and substrate-temperature effect. Journal of Applied Physics, 93, 4300–4305.

Chai, M., Brown, J.M., and Slutsky, L.J. (1997) The elastic constants of a pyrope-grossular-almandine garnet to 20 GPa. Geophysical Research Letters, 24, 523–526.

Chung, D.-H. and Lawrence, W.G. (1964) Relation of single-crystal elastic constants to polycrystalline isotropic elastic moduli of MgO: II, Temperature dependence. Journal of the American Ceramic Society, 47, 448–455.

Clarke, F.J.P., Tattersall, H.G., and Tappin, G. (1966) Toughness of ceramics and their work of fracture. Proceedings of the British Ceramic Society, 6, 163–172.

Comodi, P., Zanazzi, P.F., Poli, S., and Schmidt, M.W. (1997) High-pressure behavior of kyanite: Compressibility and structural deformations. American Mineralogist, 82, 452–459.

Conrad, P.G., Zha, C.-S., Mao, H.-K., and Hemley, R.J. (1999) The high-pressure, single-crystal elasticity of pyrope, grossular, and andradite. American Mineralogist, 84, 374–383.

Cook, R.F. and Liniger, E.G. (1992) Grain-size effects in the indentation fracture of MgO. Journal of Materials Science, 27, 4751–4761.

Cook, R.F. and Pharr, G.M. (1990) Direct observation and analysis of indentation cracking in glasses and ceramics. Journal of the American Ceramic Society, 73, 787–817.

Cook, R.F., Liniger, E.G., and Pascucci, M.R. (1994) Indentation fracture of polycrystalline cubic ceramics. Journal of Hard Materials, 5, 191–212.

Darot, M., Gueguen, Y., Benchemam, Z., and Gaboriaud, R. (1985) Ductile-brittle transition investigated by micro-indentation: results for quartz and olivine. Physics of the Earth and Planetary Interiors, 40, 180–186.

Evans, B. (1984) The effect of temperature and impurity content on indentation hardness of quartz. Journal of Geophysical Research, 89, 4213–4222.

Farber, B.Y., Orlov, V.I., and Heuer, A.H. (1998) Energy dissipation during high temperature displacement-sensitive indentation in cubic zirconia single crystals. Physica Status Solidi A, 166, 115–126.

Frischbutter, A., Neov, D., Scheffzuk, C., Vrana, M., and Walther, K. (2000) Lattice strain measurements on sandstone under load using neutron diffraction. Journal of Structural Geology, 22, 1587–1600.

Goldsby, D.L., Rar, A., Pharr, G.M., and Tullis, T.E. (2004) Nanoindentation creep of quartz, with implications for rate- and state-variable friction laws relevant to earthquake mechanics. Journal of Materials Research, 19, 357–365.

Goto, T., Ohno, I., and Sumino, Y. (1976) The determination of elastic constants of natural pyrope-almandine garnet by means of rectangular parallelepiped resonance methods. Physics of the Earth, 24, 149–158.

Gwanmesia, G.D., Liu, J., Chen, G., Kesson, S., Rigden, S.M., and Liebermann, R.C. (2000) Elasticity of the pyrope ($Mg_3Al_2Si_3O_{12}$)-majorite ($MgSiO_3$) garnets solid solution. Physics and Chemistry of Minerals, 27, 445–452.

Hartley, N.E.W. and Wilshaw, T.R. (1973) Deformation and fracture of synthetic α-quartz. Journal of Materials Science, 8, 265–278.

Ingel, R.P. and Lewis, D. (1988) Elastic anisotropy in zirconia single crystals. Journal of the American Chemical Society, 71, 265–271.

Isaak, D.G. and Graham, E.K. (1976) The elastic properties of an almandine-spessartine garnet and elasticity in the garnet solid solution series. Journal of Geophysical Research, 81, 2483–2489.

Jiang, F., Speziale, S., and Duffy, T. (2004) Single-crystal elasticity of grossular- and almandine-rich garnets to 11 GPa by Brillouin scattering. Journal of Geophysical Research, 109, B10210 (DOI: 10.1029/2004JB003081).

Karato, S., Wang, Z., Liu, B., and Fujino, K. (1995) Plastic deformation of garnets: systematics and implications for the rheology of the mantle transition zone. Earth and Planetary Science Letters, 130, 13–30.

Kessler, J.B., Ritter, J.E., and Rice, R.W. (1974) The effects of microstructure on the fracture energy of hot pressed MgO. Surface and Interface of Glasses and Ceramics, 529–544.

Lawn, B.R., Evans, A.G., and Marshall, D.B. (1980) Elastic/plastic indentation damage in ceramics: the median/radial crack system. Journal of the American Ceramic Society, 63, 574–581.

Leitner, B.J., Weidner, D.J., and Liebermann, R.C. (1981) Elasticity of single crystal pyrope and implications for garnet solid solution series. Physics of the Earth and Planetary Interiors, 22, 111–121.

Masuda, T., Hiraga, T., Ikei, H., Kanda, H., Kugimiya, Y., and Akizuki, M. (2000) Plastic deformation of quartz at room temperature: a Vickers nano-indentation test. Geophysical Research Letters, 27, 2773–2776.

Mecholsky, J.J., Freiman, S.W., and Rice, R.W. (1976) Fracture surface analysis of ceramics. Journal of Materials Science, 11, 1310–1319.

Morris, D.J. and Cook, R.F. (2005) Radial fracture during indentation by acute probes: I, description by an indentation wedging model. International Journal of Fracture, 136, 237–264.

Oliver, W.C. and Pharr, G.M. (1992) An improved technique for determining hardness and elastic modulus using load and displacement sensing indentation experiments. Journal of Materials Research, 7, 1564–1583.

O'Neill, B., Bass, J.D., Rossman, G.R., Geiger, C.A., and Langer, K. (1991) Elastic properties of pyrope. Physics and Chemistry of Minerals, 17, 617–621.

Pavese, A., Lecy, D., and Pischedda, V. (2001) Elastic properties of andradite and grossular, by synchrotron X-ray diffraction at high pressure conditions. European Journal of Mineralogy, 13, 929–937.

Rice, R.W., Freiman, S.W., and Becher, P.F. (1981) Grain-size dependence of fracture energy in ceramics: I, Experiment. Journal of the American Ceramic Society, 64, 345–350.
Soga, N. (1967) Elastic constants of garnet under pressure and temperature. Journal of Geophysics Research, 72, 4227–4234.
Tabor, D. (1956) The physical meaning of indentation and scratch hardness. British Journal of Applied Physics, 7, 159–166.
Thurn, J. and Cook, R.F. (2004) Indentation-induced deformation at ultramicroscopic and macroscopic contacts. Journal of Materials Research, 19, 124–130.
van Westrenen, W., Blundy, J., and Wood, B. (1999) Crystal chemical controls on trace element partitioning between garnet and anhydrous silicate melt. American Mineralogist, 84, 838–847.
van Westrenen, W., Blundy, J.D., and Wood, B.J. (2000) Effect of Fe^{2+} on garnet-melt trace element partitioning: experiments in FCMAS and quantification of crystal chemical controls in natural systems. Lithos, 53, 189–201.
van Westrenen, W., Wood, B.J., and Blundy, J.D. (2001) A predictive thermodynamic model of garnet-melt trace element partitioning. Contributions to Mineralogy and Petrology, 142, 219–234.
Vlassak, J.J. and Nix, W.D. (1993) Indentation modulus of elastically anisotropic half spaces. Philosophical Magazine A, 67, 1045–1056.
Wang, H. and Simmons, G. (1974) Elasticity of some mantle crystal structures, 3. Spessartite-almandine garnet. Journal of Geophysical Research, 79, 2607–2613.
Wang, Z. and Ji, S. (2001) Elasticity of six polycrystalline silicate garnets at pressure up to 3.0 GPa. American Mineralogist, 86, 1209–1218.
Weaver, J.S., Takahashi, T., and Bass, J.D. (1976) Isothermal compression of grossular garnets to 250 kbar and the effect of calcium on the bulk modulus. Journal of Geophysical Research, 81, 2475–2482.
Webb, S.L. (1989) The elasticity of the upper mantle orthosilicates olivine and garnet to 3 GPa. Physics and Chemistry of Minerals, 16, 684–692.
Westbrook, J.H. (1958) Temperature dependence of strength and brittleness of some quartz structures. Journal of the American Ceramic Society, 41, 433–440.
Whitney, D.L., Cooke, M.L., and Du Frane, S.A. (2000) Modeling of radial fracturing at corners of inclusions in garnet using fracture mechanics. Journal of Geophysical Research, 105, 2843–2853.
Winkler, B., Hytha, M., Warren, M.C., Milman, V., Gale, J.D., and Schreuer, J. (2001) Calculations of the elastic constants of the Al_2SiO_5 polymorphs andalusite, sillimanite, and kyanite. Zeitschrift fur Kristallographie, 216, 67–70.
Yang, H.X., Downs, R.T., Finger, L.W., Hazen, R.M., and Prewitt, C.T. (1997) Compressibility and crystal structure of kyanite, Al_2SiO_5, at high pressure. American Mineralogist, 82, 467–474.
Yegeneh-Haeri, A., Weidner, D.J., and Ito, E. (1990) Elastic properties of the pyrope-majorite solid solution series. Geophysical Research Letters, 17, 2453–2456.

MANUSCRIPT RECEIVED JANUARY 10, 2006
MANUSCRIPT ACCEPTED OCTOBER 3, 2006
MANUSCRIPT HANDLED BY JENNIFER THOMSON